CENTRAL INSTITUTE OF PHYSICS

INSTITUTE FOR PHYSICS AND NUCLEAR ENGINEERING

Bucharest, P.O.Box MG-6, ROMANIA

FT-325-1988 February

Protracted Releases : Inferring Source Terms and Predicting Dispersal

D.V.VAMANU*

ABSTRACT Analytical solutions are given to the transport-diffusion equation for archetype, atmospheric protracted releases featuring fronts of initiation, culminations, and tails of extinction. The interplay of the fitting parameters ensures that the model accomodate a wide typology of events, nearing in the extremes the instantaneous puff of the Lagrangian models, and the continuous stack emission of the Gaussian models, respectively. A special, though simple goniometry of field measurements of activity concentration together with a minimum of straightforward meteorological data such as the dominant wind direction and average velocity make up the input for a full analytical inferrence of such essential source terms as the time-profile of the release, the source strength, and the predicted, total dispersed activity, as well as of the diffusion coefficients that are effective in average over the time of observation and over the territory in question. The site and time of an unaccounted event having resulted in a detected atmospheric release can also be inferred through the same process. Cloud passage predictions can then be conducted. Aiming to strike some sound balance of accuracy vs.convenience of use, the approach is proposed along recent suggestions [1] that source term research be further refined, and attempts be made to improve modelling capabilities for protracted releases and dispersal. On the operative side, the models here may provide for low-cost, first-run assessments in view of early nuclear, and other industrial, alerts over large territories, thus falling in the realm of emergency preparedness and response.

*c/o National Committee for Science and Technology, 1, Piaţa Victoriei, 71202 Bucharest, Romania. Work supported by the NCST.

1. INTRODUCTION

Recent experience with radiological emergencies following severe accidents (April-May 1986 [1, 2]) has highlighted several features of such events that may require proper consideration, in view of temptatively improving nuclear emergency preparedness and crisis management procedures. Inter alia:

(i) The core and nearest field of a severe nuclear accident is very much likely to be hardly accessible at any close range for observation and measurement, which may cast serious uncertainties on the obtainability of reliable source terms. Moreover, owing to crisis constraints and crisis behaviour peculiarities, radiological emergencies originating in delayedly-reported, or even non-reported, accidents, should not be ruled out.

(ii) Considerable trans-border extension of radiological emergencies created by severe accidents fully warrant the search for reliable and expeditious procedures of source terms inferring and/or validation, at great distances from the event site, and far off the cloud/plume centreline.

(iii) There is a critical need that current procedures designed to spot, identify, characterize and predict the unfolding of abnormal nuclear events and their aftermath be further improved and better trimmed so as to provide truly assessment-under-crisis tools, within the general economy of emergency preparedness and management. In order for a procedure to qualify for safe use under crisis, it should, among others:

- be based on a versatile standard model of atmospheric releases, in the sense that the model have the capability to accomodate a comprehensive typology of events, that may effectively range from a blast (puff), to a blow, to a continuous emission; the recent wisdom [2, p.42] requires models to especially provide for satisfactory descriptions of protracted emissions, of various durations and time-profiles;

- be as selfconsistent as possible, in the sense that, for instance, some of the most critical [3] and elusive meteorological parameters -- the anisotropic diffusion coefficients -- be obtainable from the very exercise of running the model;

- be easily convertible for automated, computerized application, showing merits in terms of accuracy, speed, user-friendliness, and output expressivity; on this line, recent guidelines [3, p.62] suggest, inter alia, that first model results should be available to users within no more than 15 minutes of initiation;

- strike a better-than-average trade off between reliability and convenience of use, thereby being inexpensive and readily implementable.

In contrast with the requirements listed above, several procedures and practices recommended in literature (v.e.g. [2-5] and references) seem to vitally depend on either some satisfactory knowledge, or happy guesses, about several parameters of the event,

such as, for instance, the source strength. They also apply for distance- and time-variable diffusion parameters (standard deviations of concentration distributions) thereby invoking tables, nomograms, and somewhat loose weather descriptions associated to classes of turbulence which -- though perfectly respectable, because validated through repeated experience and wide acceptance -- still lack the required generality and are sensitive not only to specific sets of assumptions made by their authors, but also to the observer's skills. Many procedures to calculate source terms from field measurements require approaching the event site at rather close ranges, as well as the extensive use of nomograms and correlative instruments that would not easily yield to a strategy of convenient automatic calculation. Other procedures require elaborate inputs, such as full wind charts and differential temperature measurements that may take time to put together and feed into computer data files. While there is no doubt that the carefully elaborated models currently quoted in literature, and implemented in selected laboratories across the world, can yield accurate and expressive data -- provided being given in due time the appropriate input -- the recent experience seems to indicate that there may still be room for simpler, inexpensive in application, versatile and portable models that, working under a minimal set of inputs, though under what seem to be oversimplifying assumptions, can provide sound analytical and predictive first-run information on the source terms of an abnormal event resulting in an atmospheric release of radioactivity, on the effective diffusive properties of the air masses carrying it, and, on this basis, about the unfolding of the radioactive could/plume dispersal, in time and over territory, thus providing for the much sought quick response under alert.

This paper is up to proposing such an exercise.

Futile as it may seem, the effort to go all the way to solutionning the basic transport-diffusion equation for contaminated air masses would eventually prove wortn making, for in this approach it provides for a convenient hybridization of, and transparent discussion on the Gaussian diffusion (GDM), and Lagragian puff (LPM), models, with the effect of accomodating, in the same analytical expression, a comprehensive typology of releases, that may fairly cover the range between the extremes: instantaneous puff, and routine stack, emissions.

The access gained, to wide-coverage analytical solutions for the concentration of activity, opens up the possibility to track back a cloud/plume to its origin, so that to infer, through a sort of goniometry, (i) the source coordinates; (ii) the event time; (iii) the expected dispersed activity, over the entire duration o the release; (iv) the time-profile of the release; and also (v) th average coefficients of (anisotropic) downwind, cross-wind, an vertical, diffusion that were effective during the time lapse fro the event occurence through the observation moment. While the fiel collecting of goniometrical data may take some time, depending o how fast and effective the logistics involved is, the code tha solves this "inverse problem" of the atmospheric release would fal well in the range of the 15 minutes given as a comparative meri figure for such an exercise, on almost any personal computer, from few K of RAM up.

Subsequent to the inferring of the source terms and essential meteorological data is the prediction of the release unfolding -- over a territory at a given time; and in time at a given site, which would enable authorities to take the appropriate action in order to limit/alleviate the possible biological and other effects of the cloud passage. Considering the fact that the concentration of air-born activity is one crucial quantity from which a long series of derived quantities, such as the deposition, inhalation and other uptakes related to forage-cow-milk, pasture-meat, leafy vegetables etc. are obtainable [v.3], one can safely cut off the introduction of this approach at the stage of air-born concentration prediction and monitoring.

The procedure is obviously independent on the radioactive inventory at the source, for what the model handles are field measured activities, i.e. what effectively is in the air -- on what has been termed ([3], p.73) "the most critical pathway, to be quickly estimated in the early phase of an accident". Though latter iterations could profitably bring about a spectroscopic look at the problem, thus highlighting released fission products of special interest (v.[7], Appendix 9), it is believed that freeing the first-strike assessments from such delicate matters as release fractions (v.e.g. [4]) serves well the notion of an early alert and tight preparedness.

When checked against field data gathered in the months of April and May, 1986 [1,2,6,8,9] the model as proposed gave results that where satisfactory enough to encourage this line of action. Also, there are indications that the method has potential for even better approaches of the complexities of real radiological emergencies.

2. THE GENERIC MODEL FOR ATMOSPHERIC RELEASES

Let us recollect and conveniently re-phrase some basics of the physics of atmospheric releases.

In the dispersal of gases and air-born particles that make up a cloud at least three processes concur: the transport; the molecular diffusion; and the turbulent mixing. Whereas the turbulent mixing is an expression of the complex gas-dynamics and thermodynamics characteristic to large and open air masses, thus being essentially statistic in nature, the transport is clearly determined by the wind(s), and the molecular diffusion is mainly driven by concentration gradients.

In the sequel we shall work under the simplifying assumption of only two concurrent mechanisms:

(1) the wind transport, taken as a pure, horizontal, bulk translation of the entire air mass under investigation, each point at the velocity v of a dominant wind; the notion of a dominant wind implies an averaging, in both direction and magnitude, of a set of representative measurements, at different times, spots and altitudes in the region of interest (the Earth's curvature neglected); and

(ii) the diffusion -- a term that would encompass the molecular diffusion as well as the turbulent mixing and all other mechanisms that are, in a first approximation, translation-independent; the assumption goes as far as to admit that the diffusion is truly describable in terms of three diffusion coefficients, D_x, D_y, D_z, thus being in principle anisotropic with respect to the following privileged directions in space: downwind (x); cross-wind (y); and the vertical (z).

The assumptions above naturally introduce two natural reference frames in order to conveniently describe cloud dispersal:

(1) the Source System (SS), with the origin in the source of release, the OX axis downwind, the OY axis cross-wind, and the OZ axis vertical; and

(2) the Cloud System (CS), with the ox, oy, and oz axes parallel to the SS axes of respective denomination, the origin moving downwind, at the dominant wind's velocity, $\bar{v}$.

We shall consider the release of radioactivity as the aftermath of an event, of an unspecified nature, and shall take the event's inception as time origin. Consistently, in the time origin, t = 0, the SS and CS space-origins would coincide (fig.1).

The coordinates of a spot under investigation would obviously read:

$$\bar{r} = \bar{R} - \bar{v}t, \tag{2.1}$$

that is

$$\begin{aligned} x &= X - vt, \\ y &= Y \\ z &= Z \end{aligned} \tag{2.2}$$

Let V be a volume of air at rest in CS -- meaning that it moves in SS at the dominant wind velocity $\bar{v}$, and let Σ be its envelopping surface. If volume V contains, at the time t, the activity Q [Ci], then the following definitions -- all in CS -- turn out to be useful:

The concentration of activity, $\rho(\bar{r},t)$, so defined that one has

$$Q = \int_V \rho(\bar{r},t)dV, \quad [Q] = Ci, \quad [\rho] = Ci/m^3 \tag{2.3}$$

The current of activity through the surface Σ,

$$I = -\frac{\partial Q}{\partial t}, \qquad [I] = Ci/s \tag{2.4}$$

The current density, $\vec{i}$, such as

$$I = \oint_{\Sigma} \vec{i}.d\vec{s}, \qquad [i] = Ci/(m^2.s) \tag{2.5}$$

If the volume V contains also the source of the release, the generation of activity is taken care of by a source term S, such that

$$I = S - \frac{\partial Q}{\partial t}, \qquad [S] = Ci/s, \tag{2.6}$$

in relation to which a source strength, α, is defined, via the relation

$$S = \int_V \alpha dV, \qquad [\alpha] = Ci/(m^3.s) \tag{2.7}$$

Equation (2.6) expresses a balance of the activity in volume V, the first term in the right-hand side indicating generation of activity, while the second accounts for the activity loss from V through Σ. This evidently implies that the activity would observe a "conservation law" -- which, for durations in the order of hours, or even a few days, may be an acceptable first approximation.

Eventually, the length units above will be replaced by kilometers, more fit for an analysis carried out over large territories.

With the definitions above, eq.(2.6) reads:

$$\int_{\Sigma} \vec{i}.d\vec{s} = \int_V \alpha dV - \frac{\partial}{\partial t} \int_V \rho dV \tag{2.8}$$

Taking that V is rigid, the flux theorem now gives,

$$\int_V (\nabla \vec{i} + \frac{\partial \rho}{\partial t} - \alpha) dV = 0, \tag{2.9}$$

irrespective of V. Therefore,

$$\nabla \vec{i} + \frac{\partial \rho}{\partial t} = \alpha, \tag{2.10}$$

which, in CS, explicitely reads:

$$\frac{\partial i_x}{\partial x} + \frac{\partial i_y}{\partial y} + \frac{\partial i_z}{\partial z} + \frac{\partial \rho}{\partial t} = \alpha, \tag{2.11}$$

obviously with meaning of an "equation of continuity" for the activity.

At this stage one normally admits as natural the assumption that current density components obey the Fick's law:

$$i_x = -D_x \frac{\partial \rho}{\partial x},$$

$$i_y = -D_y \frac{\partial \rho}{\partial y}, \qquad (2.12)$$

$$i_z = -D_z \frac{\partial \rho}{\partial z}.$$

The diffusion coefficients D_x, D_y, D_z, that establish the proportionality of the current density with the concentration gradients are measured in m^2/s (or km^2/s, if lengths are uniformly taken in kilometers).

By carrying now the expressions (2.12) into eq.(2.11) one obtains:

$$-D_x \frac{\partial^2 \rho}{\partial x^2} - D_y \frac{\partial^2 \rho}{\partial y^2} - D_z \frac{\partial^2 \rho}{\partial z^2} + \frac{\partial \rho}{\partial t} = \alpha \qquad (2.13)$$

While in CS eq.(2.13) is a typical diffusion equation, passing to SS via the change of coordinates (2.1) would also reveal the effects of wind transport, so that in the end eq.(2.13) fully qualifies for the cloud's dispersal equation. And yet, to solve the dispersal equation it is still convenient to place oneself in CS.

At this stage it becomes evident that the power of the cloud dispersal models would very much depend on the ability to keep the source strength α, in the right-hand side of eq.(2.13), as general as possible, in order to accomodate the largest possible typology of events. One avenue to achieve this aim proved to be the solution of the dispersal equation via the mathematical Green functions associated to its differential operator in the left-hand side. On this line let us remember that, with the operator written in CS as

$$L(\bar{r},t) = -D_x \frac{\partial^2}{\partial x^2} - D_y \frac{\partial^2}{\partial y^2} - D_z \frac{\partial^2}{\partial z^2} + \frac{\partial}{\partial t} \qquad (2.14)$$

a solution of eq.(2.13) is

$$\rho(\bar{r},t) = L^{-1}(\bar{r},t)\,\alpha(\bar{r},t). \qquad (2.15)$$

By using now the Dirac functions symbolically defined as

$$\delta(\vec{r}-\vec{r}') = \delta(x-x')\delta(y-y')\delta(z-z'), \tag{2.16}$$

where

$$\delta(x-x') = \begin{cases} 0, & x' \neq x \\ \infty, & x' = x, \end{cases} \tag{2.17}$$

and

$$\int_{-\infty}^{\infty} \delta(x-x')dx' = 1, \text{ etc.}, \tag{2.18}$$

the source strength in the right-hand side of eq.(2.15) assumes the natural representation

$$a(\vec{r},t) = \int_{-\infty}^{\infty} d^3\vec{r}' \int_{-\infty}^{\infty} dt' \delta(\vec{r}-\vec{r}')\delta(t-t')a(\vec{r}',t'). \tag{2.19}$$

where the notation means:

$$\int_{-\infty}^{\infty} d^3\vec{r}' = \int_{-\infty}^{\infty} dx' \int_{-\infty}^{\infty} dy' \int_{-\infty}^{\infty} dz', \tag{2.20}$$

so that the first integral covers the whole space.

With these, the solution (2.19) reads

$$\phi(\vec{r},t) = \int_{-\infty}^{\infty} d^3\vec{r}' \int_{-\infty}^{\infty} dt' \; G(\vec{r}-\vec{r}',t-t')a(\vec{r}',t'), \tag{2.21}$$

an expression that introduces the Green function of the L operator as

$$G(\vec{r}-\vec{r}',t-t') = L^{-1}(\vec{r},t)\delta(\vec{r}-\vec{r}')\delta(t-t'). \tag{2.22}$$

Upon using the standard Fourier representation of the Dirac functions, namely

$$\begin{aligned} \delta(\vec{r}-\vec{r}') &= \frac{1}{(2\pi)^3}\int_{-\infty}^{\infty} d^3\vec{k} e^{i\vec{k}(\vec{r}-\vec{r}')}, \\ \delta(t-t') &= \frac{1}{2\pi}\int_{-\infty}^{\infty} d\chi e^{i\chi(t-t')}, \end{aligned} \tag{2.23}$$

the following integral representation of the L operator's Green function is easily obtained:

$$G(\vec{r}-\vec{r}',t-t') = \frac{1}{(2\pi)^4}\int d^3\vec{k}\int_{-\infty}^{\infty} d\chi \frac{e^{i\vec{k}(\vec{r}-\vec{r}')}\, e^{i\chi(t-t')}}{D_x k_x^2 + D_y k_y^2 + D_z k_z^2 + i\chi} \qquad (8.24)$$

The notations

$$\begin{aligned} &D_x k_x^2 + D_y k_y^2 + D_z k_z^2 = K^2 > 0, \\ &\vec{r}-\vec{r}' = \vec{r},\ t-t' = t \end{aligned} \qquad (2.25)$$

allow for writing the expression (2.24) in the form

$$G(\vec{r},t) = \frac{1}{(2\pi)^4}\int_{-\infty}^{\infty} d^3\vec{k}\, e^{i\vec{k}\vec{r}}\, g(K,t), \qquad (2.26)$$

with

$$g(K,t) = \int_{-\infty}^{\infty} d\chi \frac{e^{i\chi t}}{\chi - iK^2} \qquad (2.27)$$

The last integral is easily performed in the complex χ-plane, yielding

$$g(K,t) = \theta(t).2\pi i.e^{-K^2 t}, \qquad (2.28)$$

with θ denoting the Heaviside function:

$$\theta(t) = \begin{cases} 1, & t \geq 0 \\ 0, & t < 0 \end{cases} \qquad (2.29)$$

The result (2.28) would now bring (2.24) into a product of separate functions of x, y, and z, respectively:

$$G(\vec{r},t) = \theta(t).G_x(x,t)G_y(y,t)G_z(z,t), \qquad (2.30)$$

where, generically,

$$G_\xi(\xi,t) = \frac{1}{2\pi}\int_{-\infty}^{\infty} dk_\xi e^{ik_\xi \xi - D_\xi k_\xi^2 t}, \quad \xi = x,y,z\ . \qquad (2.31)$$

A change of variable and the use of the Poisson integral

$$\int_{-\infty}^{\infty} d\xi e^{-\xi^2} = \sqrt{\pi} \qquad (2.32)$$

readily gives

$$G(\xi,t) = \frac{1}{\sqrt{4\pi D_\xi}} \frac{e^{-\frac{\xi^2}{4D_\xi t}}}{\sqrt{t}} \quad , \xi = x,y,z \ , \tag{2.33}$$

which finally concurs to giving the analytical expression of the Green function of L:

$$G(\bar{r},t) = \theta(t) \cdot \frac{1}{(4\pi)^{\frac{3}{2}}\sqrt{D_x D_y D_z}} \cdot \frac{e^{-\frac{1}{4t}\left(\frac{x^2}{D_x} + \frac{y^2}{D_y} + \frac{z^2}{D_z}\right)}}{t^{\frac{3}{2}}} \ . \tag{2.34}$$

For the approach taken in this paper, the graphic representation in Fig.2, of the generic Green function (2.33), will prove meaningful. Also of consequence is the remark that, since

$$\lim_{D_x \to 0} G_\xi(\xi,t) = \begin{cases} 0, & x \neq 0 \\ \infty, & x = 0 \end{cases} \tag{2.34}$$

and

$$\int_{-\infty}^{\infty} G(\xi,t)d\xi = 1 , \tag{2.35}$$

the properties (2.17), (2.18) of the Dirac function are satisfied, so that one has:

$$\lim_{D_\xi \to 0} G_\xi(\xi,t) = \delta(\xi), \ \xi = x,y,z \ . \tag{2.36}$$

In particular, the following finding based on the above will be invoked in the sequel:

$$\lim_{\substack{D_x \to 0 \\ t > 0}} G(r,t) = \delta(x) \cdot \frac{1}{4\pi\sqrt{D_y D_z}} \frac{e^{-\frac{1}{4t}\left(\frac{y^2}{D_y} + \frac{z^2}{D_z}\right)}}{t} \tag{2.37}$$

Back to the solution (2.21) of the dispersal problem, considering the expressions (2.30) and (2.33) and performing the integral over the variable t, one gets:

$$\rho(x,y,z;t) \underset{(t \geq 0)}{=} \int_{-\infty}^{\infty} dx' \int_{-\infty}^{\infty} dy' \int_{-\infty}^{\infty} dz' \cdot \int_{-\infty}^{t} d\alpha' .$$

$$. \; G_x(x-x',t-t')G_y(y-y',t-t')G_z(z-z',t-t') \; . \qquad (2.38)$$

$$. \; \alpha(x',y',z';t'),$$

where

$$G(\xi-\xi',t-t') \underset{(t > t')}{=} \frac{1}{\sqrt{4\pi D_\xi}} \frac{e^{-\frac{(\xi-\xi')^2}{4D_\xi t}}}{\sqrt{t-t'}} \qquad \begin{matrix} \xi = x,y,z \\ \xi' = x',y',z' \end{matrix} . \qquad (2.39)$$

Though mathematically particular to the dispersal equation (2.13), solution (2.38,39) is general in the physical sense, because it stands as it is for an unspecified source strength, α -- which, so far, is consistent with the program announced in the Introduction. In the following section this quality will be further observed and used, to the extent possible.

On the other hand, before proceeding further it is perhaps wise to indicate how the general solution (2.38,39) relates to the well-established, conventional Gaussian, and Lagragian, models, respectively.

To obtain these it suffices to assume that the source strength is strictly singular, both in time and space, which would read, in SS:

$$\alpha(X',Y',Z';t) = Q.\delta(t').\delta(X')\delta(Y').[\delta(Z'-H)+\delta(Z'+H)] \qquad (2.40)$$

and in CS

$$\alpha(x',y',z';t') = Q\delta(t')\delta(x'+vt')\delta(y')[\delta(z'-H)+\delta(z'+H)] \qquad (2.41)$$

where again the relations (2.2) were used.

Such a source strength will immediately bring the solution (2.38) into the form

$$\rho(x,y,z;t) = Q.G_x(x,t).G_y(y,t). \\ . \; [G_z(z-H,t)+G_z(z+H,t)] \qquad (2.42)$$

Written explicitely, and taking that

$$\sigma_x = \sqrt{2D_x t}, \; \sigma_y = \sqrt{2D_y t}, \; \sigma_z = \sqrt{2D_z t} \; , \qquad (2.43)$$

the expression (2.42) is

$$\underset{t \geq 0}{\rho(x,y,z;t)} = \frac{Q}{(2\pi)^{3/2}\sigma_x\sigma_y\sigma_z} e^{-\frac{1}{2}[(\frac{x}{\sigma_x})^2 + (\frac{y}{\sigma_y})^2]} \cdot [e^{-\frac{1}{2}(\frac{z-H}{\sigma_z})^2} + e^{-\frac{1}{2}(\frac{z+H}{\sigma_z})^2}] \quad (2.44)$$

in which one recognizes the Lagragian puff (v.e.g.[3], p.66).

The expression (2.42) can also generate the conventional Gaussian plume, if one is ready to use the property (2.36) of the Green functions. Indeed, by taking, G_x to the limit $D_x \to 0$ -- meaning that the downwind diffusion is ignored -- one can easily obtain, in SS:

$$\underset{t \geq 0}{\rho(X,Y,Z;t)} = \frac{Q}{2\pi\sigma_y\sigma_z v} \cdot \delta(t - \frac{X}{v}) \cdot e^{-\frac{1}{2}(\frac{Y}{\sigma_y})^2} \cdot [e^{-\frac{1}{2}(\frac{Z-H}{\sigma_z})^2} + e^{-\frac{1}{2}(\frac{Z+H}{\sigma_z})^2}] , \quad (2.45)$$

where a well-known property of the Dirac functions was used, namely

$$\delta(X) = \delta(X-vt) = \delta[v(t - \frac{X}{v})] = \frac{\delta(t - \frac{X}{v})}{v} \quad (2.46)$$

Taking now the time-average over a time-period Δt that contains the moment X/v one obtains:

$$\bar{\rho}(X,Y,Z) = \frac{1}{\Delta t} \int_{\Delta t \ni \frac{X}{v}} \rho(X,Y,Z;t)dt = \frac{q}{2\pi\sigma_y\sigma_z v} e^{-\frac{1}{2}(\frac{Y}{\sigma_y})^2} [e^{-\frac{1}{2}(\frac{Z-H}{\sigma_z})^2} + e^{-\frac{1}{2}(\frac{Z+H}{\sigma_z})^2}] , \quad (2.47)$$

where $q = Q/\Delta t$, and σ_y, σ_z have the expressions in (2.43), taken at the moment X/v, that is -- at the strike-time corresponding to the distance X, downwind.

The expression (2.47) is immediately comparable with the solution given in ref.[3], p.63, as featuring the Gaussian model.

Reassured by the results (2.44), (2.47), let us draw now further upon the potential of the general solution (2.38,39).

3. MODELLING RELEASE PATTERNS

The very notion of a radiological emergency, or crisis presupposes an event featuring a front of initiation, a peak of culmination, and a tail of, more or less protracted, consummation. Overly general and yet essentially accurate, such a pattern transcends Physics into what can loosely be termed as common perception. It is therefore intuitively believed that a plausible, and general, image of a radioactive release that warrants the adoption of the state of emergency should present the time-profile of the Green functions featuring the dispersal problem (v.fig.2). It is a fact that Mathematical Physics endorses such an intuitive conjecture, in that it determines that Green functions are response functions for the system, when the excitation, or input, is point-like and instantaneous -- perhaps the purest, if too radical, image of a disruptive event.

One step further is to note that, since according to the considerations submitted in the Introduction the event analysis takes place at great distances from the event site, the source can be safely considered as point-like.

The conventional wisdom is that, generally, the dispersal centre of a cloud is not with the original radioactive inventory, but rather in a point (zone) placed at a certain elevation, H, known as plume rise, above the open inventory that, in our problem, is assumed at ground zero. In the said zone the released gases and particulates are carried in the act of ejection, by sheer vertical momentum and temperature gradients.

Since at great distances from the source the reflexion of the cloud from the Earth's surface can no longer be considered ideal -- owing to the fallout and other depletion mechanisms -- reflexion can, in our sort of problem, be ignored. Nevertheless, for the sake of completeness, many expressions in the following will take reflexion into account.

3,1. Models with 3-Dimensional Diffusion

One submits that, featuring the above notions and assumptions can be the following function for the source strength, written in SS:

$$\alpha(X,Y,Z;t) = \theta(t) \cdot \frac{a}{4\sqrt{\pi\beta}} \cdot \frac{e^{-\frac{1}{4\beta t}}}{t^{3/2}} \cdot e^{-\frac{v^2}{4D_x}t} \qquad (3.1.1)$$

$$\cdot\ \delta(X)\,\delta(Y)\,[\delta(Z-H) + \delta(Z+H)]\,.$$

The Heaviside function here (v.(2.29) duly indicates that the release is initiated in the time origin, and not before $t = 0$.

The second and the third -- exponential -- factors make up a function freely evoking the time-profile of the Green functions.

Two delta-factors fix the source in the horizontal plane, at $X = 0$, $Y = 0$, while in the square brackets another couple of Dirac functions point to the virtual sources of elevation H, and -H (for the reflected source) with respect to the real source.

The factor $\exp(-v^2t/(4Dx))$ has a two-fold quality. In the physical sense, it would describe a "prompt depletion at source", of the cloud, due to a more or less sharp wind-bending of the ejected matter entailing a heavy contamination of the structures (buildings, equipment etc.) at the source site -- a part of what is conventionally known as "on-site retention" (v.e.g.[3]). Commensurately, there is a diminishing in the amount of matter that would effectively reach the virtual centre of long-range dispersal, at the elevation H -- for obviously, what gets stuck at the source escapes dispersal at any further range. It is natural that the prompt depletion increase with the wind velocity, v, and with time, and decrease with at least one diffusion coefficient, for what gets promptly dispersed escapes, in its turn, wind bending.

In a mathematical sense, the somehow artificial introduction of the prompt depletion factor is again meaningful, for it provides for obtaining a compact, analytical solution of the 3-dimensional dispersal equation -- which is a very desirable pre-requisite for one endeavour in this paper: to infer source terms and the effective diffusion coefficients from field-collected data, thus inversing the dispersal problem.

The β-factor in the expression (3.1.1) is crucial in shaping the time-profile of the release. As indicated in figure 3, a larger β would place the release peak close to the release initiation at $t = 0$, while also narrowing the width, and we are thus watching a <u>blast</u> (puff), or explosive release. At moderate β one faces a <u>blow</u>, whereas at smaller β the pattern of a quasi-continuous release could be fairly approached, particularly at low wind velocities. Figure 3 may give a better perception of these features. In all cases, α will fitfully second β in fixing the profile <u>and</u> amplitude of the release.

Dimensionally, as long as

$$[\alpha(x,y,z;t)] = Ci/(m^3.s) \text{ and } [\delta] = m^{-1}, \qquad (3.1.2)$$

one has

$$[\beta] = s^{-1} \text{ and } [\alpha] = Ci \tag{3.1.3}$$

Starting from the physical meaning of the source strength (v.section 2), it is clear that, by integrating it over the entire space and time, one must obtain the total activity dispersed during the release. One finds, successively:

$$\int_{-\infty}^{\infty} dx \int_{-\infty}^{\infty} dy \int_{-\infty}^{\infty} dz \cdot \int_{-\infty}^{\infty} dt\, a(x,y,z;t) = \tag{3.1.4}$$

$$= \frac{1}{2} \cdot a \int_{-\infty}^{\infty} \frac{e^{-\frac{1}{4\tau}}}{\sqrt{\pi}\tau^{3/2}} \cdot e^{-\frac{v^2}{4\beta D_x}\tau} d\tau ,$$

where the change of variable $\tau = \beta t$ has been used. Noting that the integral in the right-hand side of the identity (3.1.4) is the Laplace transform of the first factor, in the end one finds the total dispersed activity, a_d:

$$a_d = a e^{-\frac{v}{2\sqrt{\beta D_x}}} . \tag{3.1.5}$$

By writing the source strengtn (3.1.1) in CS and taking into account the effects of the Dirac and Heaviside functions, the activity concentration (2.38) now reads:

$$\underset{(t > 0)}{\rho(x,y,z;t)} = \frac{a}{4\sqrt{\pi\beta}} \int_0^t dt' \frac{e^{-\frac{1}{\beta t'}}}{t'^{3/2}} e^{-\frac{v^2}{4D_x}t'} \cdot \tag{3.1.6}$$

$$\cdot G_x(x+vt', t-t') G_y(y, t-t') \cdot [G_z(Z-H, t-t') + G_z(Z+H, t-t')] ,$$

With a change of variable,

$$t - t' = \tau , \tag{3.1.7}$$

and returning to SS, also giving the Green functions their full expression one obtains

$$\rho(X,Y,Z;t) \underset{(t \geq 0)}{=} \frac{q}{8\pi\sqrt{8.D_x D_y D_z}} \cdot e^{\frac{v}{2D_x} X} \cdot \qquad (3.1.8)$$

$$\cdot \left\{ \int_0^t d\tau \, \frac{e^{-\frac{1}{4\beta(t-\tau)}}}{\sqrt{\pi}(t-\tau)^{3/2}} e^{-\frac{v^2}{4D_x}(t-\tau)} \cdot \right.$$

$$\cdot \frac{e^{-\frac{1}{4\tau}\left[\frac{X^2}{D_x} + \frac{Y^2}{D_y} + \frac{(Z-H)^2}{D_z}\right]}}{\sqrt{\pi}\,\tau^{3/2}} e^{-\frac{v^2}{4D_x}\tau} +$$

$$\left. + \int_0^t d\tau \, \frac{e^{-\frac{1}{4\beta(t-\tau)}}}{\sqrt{\pi}\,(t-\tau)^{3/2}} e^{-\frac{v^2}{4D_x}(t-\tau)} \cdot \frac{e^{-\frac{1}{4\tau}\left[\frac{X^2}{D_x} + \frac{Y^2}{D_y} + \frac{(Z+H)^2}{D_z}\right]}}{\sqrt{\pi}\,\tau^{3/2}} e^{-\frac{v^2}{4D_x}\tau} \right\}.$$

In the above integrals one can recognize the convolution of the functions

$$f(\tau) = \frac{e^{-\frac{A(\pm H)^2}{4\tau}}}{\sqrt{\pi}\,\tau^{3/2}} e^{-\frac{v^2}{4D_x}\tau}, \qquad (3.1.9)$$

and

$$g(t-\tau) = \frac{e^{-\frac{1}{4(t-\tau)}}}{(t-\tau)^{3/2}} e^{-\frac{v^2}{4D_x}(t-\tau)}, \qquad (3.1.10)$$

where it has been convenient to write:

$$A(\pm H) = \sqrt{\frac{X^2}{D_x} + \frac{Y^2}{D_y} + \frac{(Z \pm H)^2}{D_z}} \qquad (3.1.11)$$

Another useful notation is

$$I(X,Y,Z\pm H;t) = \int_0^t d\tau f(\tau).g(t-\tau), \qquad (3.1.12)$$

with which the expression (3.1.8) reads:

$$\rho(X,Y,Z;t) \underset{(t \geq 0)}{=} \frac{a}{32\pi\sqrt{\beta}.D_x D_y D_z} \cdot e^{\frac{v}{2D_x}X} \cdot [I(X,Y,Z-H;t) + I(X,Y,Z+H;t)] \qquad (3.1.13)$$

It is common knowledge that the Laplace transforms of the convolutions take the simple form:

$$L[I] = f(s)g(s), \qquad (3.1.14)$$

where

$$f(s) = \frac{2}{A(\pm H)} e^{-A(\pm H)\sqrt{s + \frac{v^2}{4D_x}}} \qquad (3.1.15)$$

$$g(s) = \frac{2}{\frac{1}{\sqrt{\beta}}} e^{-\frac{1}{\sqrt{\beta}}\sqrt{s + \frac{v^2}{4D_x}}} \qquad (3.1.16)$$

are the Laplace images of the functions (3.1.9,10), derived from the original [exp $(-1/(4\tau))/(\sqrt{\pi}\,\tau^{3/2})$, after the original had undergone a translation by a factor of $\exp(-v^2/(4D_x\tau))$.

Upon these remarks one immediately finds

$$L[I] = 2\left[\frac{1}{A(\pm H)} + \sqrt{\beta}\right] \cdot \frac{2}{A(\pm H) + \frac{1}{\sqrt{\beta}}} e^{-\left[A(\pm H)+\frac{1}{\sqrt{\beta}}\right]\sqrt{s + \frac{v^2}{4D_x}}} \qquad (3.1.17)$$

It is precisely this expression which provides for the identification as original of this Laplace image, of the function

$$I(X,Y,Z\mp H;t) = 2\left[\frac{1}{A(\mp H)} + \sqrt{\beta}\right] \cdot \qquad (3.1.18)$$

$$\cdot \frac{e^{-\frac{1}{4t}\left[A(\mp H) + \frac{1}{\sqrt{\beta}}\right]^2}}{\sqrt{\pi}\, t^{\frac{3}{2}}} \cdot e^{-\frac{v^2}{4D_x} t}$$

Note that such a smooth handling of the Laplace transformation would have been hardly possible, had the prompt depletion factor been ignored in the expression (3.1.1) of the source strength.

By carrying this result in the expression (3.1.13), the activity concentration in this 3-dimensional dispersal model finally reads (in SS):

$$\rho(X,Y,Z;t) = \frac{a}{16\pi^{\frac{3}{2}}\sqrt{\beta D_x D_y D_z}} \cdot \frac{e^{\frac{v}{2D_x}X - \frac{v^2}{4D_x}t}}{t^{\frac{3}{2}}} \cdot$$

$$\left\{ \cdot \left(\sqrt{\beta} + \frac{1}{\sqrt{\frac{X^2}{D_x} + \frac{Y^2}{D_y} + \frac{(Z-H)^2}{D_z}}}\right) \cdot e^{-\frac{1}{4t}\left[\frac{1}{\sqrt{\beta}} + \sqrt{\frac{X^2}{D_x} + \frac{Y^2}{D_y} + \frac{(Z-H)^2}{D_z}}\right]^2} \right. \qquad (3.1.19)$$

$$\left. + \left(\sqrt{\beta} + \frac{1}{\sqrt{\frac{X^2}{D_x} + \frac{Y^2}{D_y} + \frac{(Z+H)^2}{D_z}}}\right) \cdot e^{-\frac{1}{4t}\left[\frac{1}{\sqrt{\beta}} + \sqrt{\frac{X^2}{D_x} + \frac{Y^2}{D_y} + \frac{(Z+H)^2}{D_z}}\right]^2} \right\} .$$

The expression (3.1.19) has been extensively tested numerically only to conclude that it can provide ample coverage for a large variety of releases, differing in time-shape and amplitude. Two kind of tests have been performed: (i) cloud patterns mapped over territory at given times; and (ii) time-profiles of the concentration at a given spot. Figures 4 and 5 are samples of the respective kinds.

3.2. Models with 2-Dimensional Diffusion

There are several reasons warranting the use of the framework given in section 2 for designing also a two-dimensional dispersal model. The first, and obvious, is that 2-d models enjoy a wide acceptance in the concerned literature, so that it may be proper to have the specific considerations in this paper also tailored for the accepted wisdom, and practice. The less obvious, though perhaps more important, reason, is that -- at least at present -- the solution of the dispersal inverse problem can apply to the 3-d model in section 3.1 only in cases that the cloud's centreline can be directly accessed for monitoring and measurements. Since the author's approach here is to always consider the least favourable circumstances, a procedure should be made available also for cases when the cloud's centreline in not directly accessible, which would mean, for instance, that the source site is off the national territory, and the wind direction is such that the centreline does not cross the borders, though the national territory is in the downwind half-plane with respect to the source. It turns out that a 2-d model can be brought to solve the inverse problem in such a case.

In contrast with the customary practice of treating two-dimensional plumes originating in continuous stack emissions, the model here will take up again the archtype of a release as described in the introduction of section 3.

Accordingly, for the source strength the following function is proposed (in SS):

$$\alpha(X,Y,Z;t) = \theta(t) \cdot \frac{\alpha}{2\sqrt{\pi\beta}} \cdot \frac{e^{-\frac{1}{\beta t}}}{t^{\frac{3}{2}}} \cdot \delta(X)\delta(Y) \cdot \qquad (3.2.1)$$

$$\cdot \left[\delta(Z-H) + \delta(Z+H)\right] .$$

For the meaning assigned to the various factors in the expression above, the reader is referred to the comments on the expression (3.1.1). The only major difference in the 2d case regards the absence of the "prompt depletion" factor. Since the latter is connected to the downwind diffusion -- which is precisely the aspect that is neglected in a two-dimensional Gaussian plume -- the said absence is certainly understandable.

All the other requirements for a source strength are satisfied. In particular, one can see that function (3.2.1) is Green-like, with a maximum at

$$t_m = \frac{2}{3\beta} , \qquad (3.2.2)$$

reaching

$$q_m = \frac{3}{4e}\sqrt{\frac{3}{e\pi}}\,\alpha\beta \quad , \tag{3.2.3}$$

adjustable to a comprehensive typology of releases (figure 6).

Again a full integration over space and time gives the total dispersed activity:

$$\int_{-\infty}^{+\infty} dX \int_{-\infty}^{+\infty} dY \int_{-\infty}^{+\infty} dZ \cdot \int_{-\infty}^{+\infty} dt\; a(X,Y,Z;t) = a \quad , \tag{3.2.4}$$

thus revealing the meaning of a.

Writing the source (3.2.1) in CS, then carrying it into the general expression (2.38) of the activity, calculations similar to those in section 3.1 would give

$$\rho(X,Y,Z;t) = \frac{a}{2\sqrt{\pi\beta}} \int_{o}^{t} d\tau\, \frac{e^{-\frac{1}{\beta(t-\tau)}}}{(t-\tau)^{\frac{3}{2}}} \tag{3.2.5}$$
$$(t \geq 0)$$

$$\cdot\, G_X(X-v\tau,\tau)\,G_Y(Y,\tau)\cdot[G_Z(Z-H,\tau) + G_Z(Z+H,\tau)]\,,$$

with the appropriate Green functions given by

$$G_\xi(\xi,\tau) = \frac{1}{\sqrt{4\pi D_\xi \tau}}\, e^{-\frac{\xi^2}{4D_\xi\tau}} \quad . \tag{3.2.6}$$

Since the integral in the expression (3.2.5) would not yield easily to the attempts of having it performed analytically, the alternative approach proposed in the following will transform the genuinely three-dimensional formula (3.2.5) into a two-dimensional one.

The alternative consists in neglecting the downwind diffusion, which mathematically reads:

$$D_X = 0 \tag{3.2.7}$$

One can recall now the property (2.36) of the Green functions, indicating that

$$\lim_{D_X \to 0} G_x(X-v\tau,\tau) = \delta(X-v\tau) = \delta[v(\frac{X}{v} - \tau)] = \frac{\delta(\tau - \frac{X}{v})}{v} \qquad (3.2.8)$$

where the property (2.46) of the Dirac functions was again used.

Consequently, the expression (3.2.5) of the activity concentration becomes:

$$\rho(X,Y,Z;t) = \frac{a}{2\sqrt{\pi}\beta v} \int_0^t d\tau \frac{e^{-\frac{1}{\beta(t-\tau)}}}{(t-\tau)^{\frac{3}{2}}} \delta(\tau - \frac{X}{v}) \cdot \qquad (3.2.9)$$

$$\cdot\ G_y(Y,\tau)[G_z(Z-H),\tau) + G_z(Z+H,\tau)] \ .$$

The Dirac function under the integral prompts the following remark:

$$\text{For } X > 0 \text{ (downwind)}: \begin{cases} \text{if } 0 \le \frac{X}{v} \le t, \text{ then } \rho \neq 0; \\ \text{if } t < \frac{X}{v}, \qquad\qquad \rho = 0, \end{cases} \qquad (3.2.10)$$

which requires in the expression of the concentration a Heaviside factor

$$\theta(t - \frac{X}{v}) = \begin{cases} 1, \ \frac{X}{v} \le t \\ 0, \ t < \frac{X}{v} \end{cases} \qquad (3.2.11)$$

For $X < 0$: always $\rho = 0$,
(upwind)

which in turn requires another Heaviside factor

$$\theta(X) = \begin{cases} 1, \ X \ge 0 \\ 0, \ X < 0 \ . \end{cases} \qquad (3.2.12)$$

or, alternatively, a firm specification that the expression for the activity concentration refers only to the half-plane X > 0. Thus the major shortcoming of any 2-d model becomes apparent: it cannot properly describe dispersal at, and near, the source of release. In particular, according to any 2-d model there is no upwind diffusion at all, no matter how low the wind velocity -- which certainly contradicts the experience. Fortunately enough, this aspect is of little consequence for the dispersal over distant territories -- which makes the major issue of this paper.

Upon the remarks above, and using the explicit expressions of the Green functions one finds:

$$\rho(X,Y,Z,t) = \theta(t - \frac{X}{v}) \cdot \frac{q}{8\pi\sqrt{\pi\theta D_y D_z}} \cdot \frac{1}{X} \cdot \frac{e^{-\frac{1}{\theta(t-\frac{X}{v})}}}{(t-\frac{X}{v})^{3/2}} \cdot \quad (3.2.13)$$
$$t \geq 0$$
$$X > 0$$

$$\cdot e^{-\frac{v}{4D_y}\frac{Y^2}{X}} \left[e^{-\frac{v}{4D_z}\frac{(Z-H)^2}{X}} + e^{-\frac{v}{4D_z}\frac{(Z+H)^2}{X}} \right].$$

The remaining Heaviside factor above illustrates one feature of the 2-d models: the strike time,

$$t_s = \frac{X}{v} , \quad (3.2.14)$$

implying that no effect of the release is to be felt along the wind front at a distance X from the source but after a time lapse t_s, measured from the adopted time origin -- the moment of the release inception.

Like its 3-dimensional counterpart (3.1.19), the expression (3.2.13) has been tested as far as cloud patterns and time-profiles. To illustrate, samples are given in figures 7 and 8.

4. THE INVERSE PROBLEM

With two alternative analytical expressions (3.1.19) and (3.2.13) for the activity concentration now handy, one can proceed to question source terms and effective diffusion coefficients, based on field data.

The operation's sequence starts by a meteorlogical inquiry, during which as many as possible meteo stations covering the territory of interest are requested to indicate the dominant wind velocity and direction at their respective sites. At the headquarters managing the crisis an average is then taken over these, to determine the velocity and direction of a single, reference, dominant wind.

In a second phase a reconnaissance plane, with exposure meters on-board is directed to fly cross-wind, and at various altitudes, in order to pinpoint the cloud centreline -- by taking the maximum readings both cross-wind and vertically. Relevant ground marks for the centreline and its elevation are to be reported at headquarters. In the event that over the entire territory that can be accessed by a crosswind flight one cannot reach a maximum reading for the exposure, then it must be inferred that the centreline does not cross the respective territory, extending outside its borders along the dominant wind in the general direction of the increasing readings. However, even in this case the centreline elevation can be determined as lying at the height of the maximum exposure reading along a vertical -- which is consistent with the nature of the solutions (3.1.19) and (3.2.13).

At this stage the procedure splits. If centreline crosses accessible territory (direct blow), the 3-dimensional dispersal model can be used. If centreline falls off the borders (indirect blow) the use of the 2-dimensional model is in order.

4.1. Direct Blow

In case of a direct blow the inference procedure would require that five planes, equipped with the appropriate instrumentarium to measure activity concentration in air, perform three consecutive flights, all cross-wind, and crossing the cloud centreline in the configuration depicted in figure 9. The three hours T_1, T_2, and T_3, at which the air is to be probed would be chosen so that

$$T_3 - T_2 = T_2 - T_1 \ . \qquad (4.1.1)$$

If T_o is the hour to mark the time origin, i.e. the release inception, then or course

$$T_j - T_o = t_j, \quad j = 1,2,3 \qquad (4.1.2)$$

would relocate the measurements in the event's time scale.

We will persistently assume that the source is distant from the theatre of inferrence. Accordingly, the cloud reflection is to be neglected. By the same token one can safely assume that the barometric altitudes of the source, and landmark of the measuring unit M_o are enough comparable in actuality, to be taken as identical in calculations.

As soon as the results of the measurements on the activity concentration become available, the headquarters can build up the following table of inputs:

a) Meteo: - dominant wind direction, u (radians, from North by East
- dominant wind velocity, v (km/h)

b) Cloud: - centreline ground marks
- centreline elevation (km)

c) Flight-scan (v.fig.7)

Table 1

Measuring unit	Time T_1	T_2	T_3
$M_o(X_o,O,H)$	ρ_{01}	ρ_{02}	ρ_{o3}
$M_1(X_o+d,O,H)$	ρ_{11}	ρ_{12}	ρ_{13}
$M_2(X_o+2d,O,H)$	ρ_{21}	ρ_{22}	-
$M'_o(X_o,O,H+h)$	ρ'_{01}	ρ'_{02}	-
$M''_o(X_o,d,H)$	ρ''_{01}	ρ''_{02}	-

The strike time T_s at M_o (v.(3.2.14) and comments) is to join this table.

The coordinates of the measuring units are taken in SS.

In units consistent with the magnitude of the investigated field, it is convenient that the distances d and h between the measuring units be expressed in km, and the activity concentrations ρ, in Ci/km^3.

As indicated in the following, the quantities under the headings a), b), and c), suffice for inferring:

(i) the source terms, according to the adopted model:

- release time, T_o (h)
- source site, X_o (km. v.also fig.9)
- total dispersed activity, a_d (Ci, v.(3.1.5)), and the associated source strength coefficient, α ($Cf/(km^3.s)$)
- blast factor (release's time-shape factor), β (s^{-1})

(ii) the effective diffusion coefficients, D_x, D_y, D_z (km^2/s)

The first step towards founding the inferring procedure is to construct the expressions for the field data gathered in the flight-scan table 1, starting from the general expression (3.1.19), for the activity concentration. Brought to a form convenient for an easy reading of the calculations, the respective expressions are given in the Appendix 1.

Taking the ratios and logarithms indicated in the left-hand site of the expression that follows one obtains:

$$\ln\left(\frac{\rho_{13}}{\rho_{12}} \cdot \frac{\rho_{02}}{\rho_{03}}\right) = \frac{1}{4D_x}\frac{t_3-t_2}{t_2t_3}\left[\left(\sqrt{\frac{D_x}{\beta}} + X_o + d\right)^2 - \left(\frac{D_x}{\beta} + X_o\right)^2\right] \quad (4.1.1)$$

$$\ln\frac{\rho_{12}}{\rho_{11}} \cdot \frac{\rho_{01}}{\rho_{02}} = \frac{1}{4D_x}\frac{t_2-t_1}{t_1t_2}\left[\left(\sqrt{\frac{D_x}{\beta}} + X_o + d\right)^2 - \left(\frac{D_x}{\beta} + X_o\right)^2\right]. \quad (4.1.2)$$

Taking now the ratio of the above, noting that

$$t_3 - t_2 = t_2 - t_1, \quad (4.1.3)$$

using the notations

$$L_{01}^{12} = \ln\left(\frac{\rho_{12}}{\rho_{11}} \cdot \frac{\rho_{01}}{\rho_{02}}\right), \quad L_{01}^{23} = \ln\left(\frac{\rho_{13}}{\rho_{12}} \cdot \frac{\rho_{02}}{\rho_{03}}\right),$$

$$N_{01}^{123} = \frac{L_{01}^{12}}{L_{01}^{23}}, \quad (4.1.4)$$

also using the remark (4.1.3), the <u>release time</u> T_o is obtained in the form

$$T_o = \frac{T_3 - T_1 \cdot N_{01}^{123}}{1 - N_{01}^{123}} \quad (R.1)$$

Similarly, from

$$\ln\left(\frac{\rho_{12}}{\rho_{11}} \cdot \frac{\rho_{01}}{\rho_{02}}\right) = \frac{1}{4D_x} \cdot \frac{t_2-t_1}{t_1 t_2} \left[\left(\sqrt{\frac{D_x}{\beta}} + X_o + d\right)^2 - \left(\frac{D_x}{\beta} + X_o\right)^2\right] \quad (4.1.5)$$

$$\ln\left(\frac{\rho_{22}}{\rho_{21}} \cdot \frac{\rho_{01}}{\rho_{02}}\right) = \frac{1}{4D_x} \cdot \frac{t_2-t_1}{t_1 t_2} \left[\left(\sqrt{\frac{D_x}{\beta}} + X_o + 2d\right)^2 - \left(\frac{D_x}{\beta} + X_o\right)^2\right] \quad (4.1.6)$$

one derives

$$\sqrt{\frac{D_x}{\beta}} + X_o = d \frac{4M_{012}^{12} - 1}{2(1-2M_{012}^{12})} , \quad (4.1.7)$$

where

$$M_{012}^{12} = \frac{\ln\left(\frac{\rho_{12}}{\rho_{11}} \cdot \frac{\rho_{01}}{\rho_{02}}\right)}{\ln\left(\frac{\rho_{22}}{\rho_{21}} \cdot \frac{\rho_{01}}{\rho_{02}}\right)} = \frac{L_{01}^{12}}{L_{02}^{12}} \quad (4.1.8)$$

The result (4.1.7) is indeed useful, since in combination with (4.1.2) it yields the downwind diffusion coefficient:

$$D_x = \frac{T_2-T_1}{(T_1-T_o)(T_2-T_o)} \cdot \frac{d^2}{2L_{01}^{12}} \cdot \frac{M_{012}^{12}}{1 - 2M_{012}^{12}} . \quad (R.2)$$

Taking now the ratio ρ_{01}/ρ_{11} and making use of the partial result (4.1.7) one obtains

$$X_o = \frac{d}{\frac{\rho_{01}}{\rho_{11}} \cdot \frac{\exp\left\{-\frac{T_2-T_o}{T_1-T_2} L_{01}^{12}\left[1-\frac{v}{d}(T_1-T_o)\frac{1-2M_{012}^{12}}{M_{012}^{12}}\right]\right\}}{4M_{012}^{12} - 1} - 1} . \quad (R.3)$$

which obviously suffices to identify the site of the release source (v.fig.7).

Upon the knowledge of D_x and X_o, again from (4.1.7) the blast factor is derived:

$$\beta = D_x / \left[d \frac{4M_{012}^{12} - 1}{2(1 - 2M_{012}^{12})} - X_o \right]^2 \qquad (R.4)$$

To get the appropriate expression for the vertical diffusion coefficient one has to explicitely construct now the ratio ρ'_{02}/ρ'_{01}, based on the respective expressions in Appendix 1. Similarly, one obtains D_y starting from ρ''_{02}/ρ''_{01}:

$$D_z = \frac{h^2}{\left\{ 2\sqrt{\frac{(T_1-T_o)(T_2-T_o)}{T_2-T_1}} \left\{ \ln\left(\frac{T_2-T_o}{T_1-T_o} \right)^{\frac{3}{2}} \cdot \frac{\rho'_{02}}{\rho'_{01}} + \frac{v^2}{4D_x}(T_2-T_1) \right\} - \frac{1}{\sqrt{\beta}} \right\}^2 - \frac{X_o^2}{D_x}} \qquad (R.5)$$

$$D_y = \frac{h^2}{\left\{ 2\sqrt{\frac{(T_1-T_o)(T_2-T_o)}{T_2-T_1}} \left\{ \ln\left(\frac{T_2-T_o}{T_1-T_o} \right)^{\frac{3}{2}} \cdot \frac{\rho''_{02}}{\rho''_{01}} + \frac{v^2}{4D_x}(T_2-T_1) \right\} - \frac{1}{\sqrt{\beta}} \right\}^2 - \frac{X_o^2}{D_x}} \qquad (R.6)$$

Re-writing now the analytic expression for ρ_{01} so that all known quantities be properly emphasized, the source strength parameter is obtained in the form:

$$\alpha = 16\pi^{\frac{3}{2}} \sqrt{D_x D_y D_z}\, (T_1-T_o)^{\frac{3}{2}} \frac{X_o}{\sqrt{\frac{D_x}{\beta}} + X_o} \cdot$$
$$\cdot \exp\left\{ \frac{v^2}{4D_x}(T_1-T_o) - \frac{v}{2D_x} X_o + \frac{1}{4(T_1-T_o)D_x} \left(\sqrt{\frac{D_x}{\beta}} + X_o \right)^2 \right\} \cdot \rho_{01} \qquad (R.7)$$

It leaves us one step from determining the total dispersed activity,

$$\alpha_d = \alpha e^{-\frac{v^2}{2\sqrt{\beta D_x}}}, \qquad (R.8)$$

which actually repeats eq.(3.1.5)

The results (R.1...8) provide the solution of the inverse problem, according to the 3-dimensional dispersal model proposed, once the input tables (a), (b), (c) are made available through field measurements.

Numerical simulations that were carried out in order to test the ability of this scheme to really infer source terms and effective diffusion coefficients have indicated that the procedure works quite satisfactorily. One problem is, of course, its sensitivity to the accuracy attained in gathering the field data, particularly having in mind the non-linear nature of the many functions involved. It turned out that, though sensitive indeed to the accuracy in measuring the input data, the solution R.1-8 is good enough, to the effect of providing for an informed decision on a nuclear alert.

4.2. *Indirect Blow*

In case of an indirect blow the inference procedure would require seven planes to probe the air in order to gather input data -- which is natural considering the need to determine one more coordinate, Y_o, that, together with X_o, will help pinpointing the source site. The flight plan is depicted in fig.10. On the other hand, it turns out that a single measurement, at a given time, provides enough input data to enable the inferrence. On the assumption of a distant source, again the cloud reflection is neglected, along with the difference in barometric altitude between the source and the ground zero of the measuring unit M_o at the moment of the measurement.

While sections (a) and (b) in the table of inputs given in paragraph 4.1 are of equal use in the case now in question, the flight scan results in section (c) have a different look, namely

(c') Flight-scan (v.fig.10)

Table 2

Measuring unit	reporting
$M_o(X_o, Y_o, H)$	ρ_o
$M'_o(X_o, Y_o, H+h)$	ρ'_o
$M_1(X_o, Y_o+d, H)$	ρ_1
$M_2(X_o, Y_o+2d, H)$	ρ_2
$M_3(X_o+d, Y_o, H)$	ρ_3
$M'_3(X_o+d, Y_o, H+h)$	ρ'_3
$M_4(X_o+d, Y_o+d, H)$	ρ_4

Skipping the comments that are similar to those in section 4.1, let us proceed to the search for the relevant quantities, using the analytic expressions given in Appendix 2, of the activity concentrations that appear in the table of inputs.

Much in the same vein as in the preceding paragraph, one write explicitely the ratios ρ_o/ρ_1 and ρ_o/ρ_2, to build then the expression

$$\frac{\ln \frac{\rho_o}{\rho_1}}{\ln \frac{\rho_o}{\rho_2}} = \frac{2Y_o + d}{2(2Y_o + 2d)} \quad . \tag{4.2.1}$$

With the notations

$$L_{01} = \ln \frac{\rho_o}{\rho_1}, \; L_{02} = \ln \frac{\rho_o}{\rho_2} \; , \tag{4.2.2}$$

some simple algebra gives

$$Y_o = \frac{1}{2} d \frac{L_{02} - 4L_{01}}{2L_{01} - L_{02}} \quad . \tag{R.9}$$

In the next step one takes

$$\frac{\rho_o}{\rho_o'} = e^{\frac{v}{4D_z} \frac{h^2}{X_o}} \; , \tag{4.2.3}$$

so that

$$D_z X_o = \frac{vh^2}{4L_{00}} \; , \tag{4.2.4}$$

where, in style with the preceeding paragraph,

$$L_{oo} = \ln \frac{\rho_o}{\rho_o'} \quad . \tag{4.2.5}$$

On the other hand, one has

$$\frac{\rho_3}{\rho_3'} = e^{\frac{v}{4D_z}\frac{h^2}{X_o+d}} \quad , \tag{4.2.6}$$

so that

$$D_z\ (X_o+d) = \frac{vh^2}{4L_{33}} \quad , \tag{4.2.7}$$

where

$$L_{33} = \ln \frac{\rho_3}{\rho_3'} \quad . \tag{4.2.8}$$

Subtracting from one another the expressions (4.2.4) and (4.2.7) one finds the vertical diffusion coefficient:

$$D_z = \frac{vh^2}{4d}\left(\frac{1}{L_{33}} - \frac{1}{L_{00}}\right). \tag{R.10}$$

Carrying this result back in the expression (4.2.4) one obtains

$$X_o = \frac{d}{\frac{L_{00}}{L_{33}} - 1} \quad , \tag{R.11}$$

which, togetner with Y_o (R.9) pinpoints the source site: the source is to be searched Y_o kilometers cross-wind from M_o in the sense of increasing concentrations, and then X_o kilometers upwind.

As soon as X_o is known, the release time of origin T_o can be readily inferred:

$$T_o = T_s - \frac{X_o}{v} \quad . \tag{R.12}$$

Another relevant couple of ratios is ρ_o/ρ_1, wherefrom

$$D_y X_o = \frac{vd(2Y_o+d)}{4L_{01}} \quad , \tag{4.2.9}$$

and ρ_3/ρ_4, which gives

$$D_y(X_o+d) = \frac{vd(2Y_o+d)}{4L_{34}} \quad , \tag{4.2.10}$$

where, similar to the notations above,

$$L_{34} = \ln \frac{\rho_3}{\rho_4} \quad . \tag{4.2.11}$$

By subtracting (4.2.9) and (4.2.10) from one another one finds

$$D_y = \frac{v(2Y_o+d)}{4} \left(\frac{1}{L_{34}} - \frac{1}{L_{01}} \right) \quad . \tag{4.2.12}$$

To get the expression for the blast factor ϕ one has first to take ρ_o/ρ_3. By substituting in the respective expression $T-T_o$ for t (T -- the measurement hour, T_o -- the event hour), one can extract

$$\beta = \frac{\dfrac{1}{T - T_o - \dfrac{X_o+d}{v}} - \dfrac{1}{T - T_o - \dfrac{X_o}{v}}}{\ln\left[\dfrac{X_o}{X_o+d}\left(\dfrac{T-T_o-\dfrac{X_o}{v}}{T-T_o-\dfrac{X_o+d}{v}}\right)^{\frac{3}{2}} \cdot \dfrac{\rho_o}{\rho_3}\right] + \dfrac{vY_o^2}{4D_y}\left(\dfrac{1}{X_o} - \dfrac{1}{X_o+d}\right)} \quad . \qquad (R.13)$$

Finally, from the very expression for ρ_o in the Appendix 2 one finds

$$a = 8.\pi\sqrt{\pi\beta D_y D_z}.\ X_o\left(T-T_o-\frac{X_o}{v}\right)^{\frac{3}{2}} e^{\beta\left(T-T_o-\frac{X_o}{v}\right)} . e^{\frac{v}{4D_y}\frac{Y_o^2}{X_o}} . \rho_o \ , \qquad (R.14)$$

with all quantities in the right-hand side known.

Results (R.9-14) make up the solution of the inverse problem according to the 2-dimensional dispersal model. The numerical simulations that were carried out warrant remarks that fully parallel those concluding the paragraph 4.1.

The overall solution (R.1-14) of the inverse problem can be, of course, subject to the standard refinements concerning the fallout, precipitation washdown, and radioactive decay, deplotions. This paper would rather not pause on these, to avoid an out-of-place change of emphasis.

5. CONCLUSION

The present paper is largely a reaction to several needs that were perceived during the radiological emergency in Europe, April, 1986.

An attempt is made, to propose an easy-to-handle, self-consistent, comprehensive and versatile model for protracted atmospheric releases, that would serve the straightforward pruposes of an early alert over large territories.

Two constructs among others are of essence towards this aim: (i) a design for the model source strength which, featuring a front of attack, a culmination, and a tail of extinction, is thought to

better accomodate the notion of a disruptive nuclear event -- that seem to entail protracted releases -- in comparison with either the instantaneous, Lagrangian, blasts or the indefinitely, Gaussian, continuous emissions that make the usual references; and (ii) a full, and expeditious, first-run solution for the inverse problem of spotting, identifying, and independently characterizing a source of radioactive release, thus enabling subsequent predictions on cloud dispersals, consequent environmental alterations, potential damage and hazards, which in turn would help taking sound decisions pertaining to crisis management.

The numerical simulations that were conducted in order to assess whether an acceptable balance of accuracy vs. conveniency of use has been reached, were encourageing.

It is believed that the idea of re-marking more complex approaches of Lagrangian type using as elemental components long-tail signals of the kind proposed here might prove worth pursueing.

Acknowledgements

The topics dealt with in this paper are part of a Programme coordinated by Professor Ioan Ursu. The author is much indebted to the Programme's leader, whose advice, assessments on the progress with this work, direct encouragement and substantive assistance were of essence in the realization of this project.

Thanks are expressed to prof.M.Oncescu and Dr.D.Galeriu for critically reading a preliminary, extended version of this manuscript, which has produced helpful suggestions, and to Dr.P.Sandru, Dr.P.Popa, Dr.L.Grigorescu, Dr.V.Zoran, and Dr.I.Draghici, for stimulating discussions.

References

1. USSR State Committee on the Utilization of Atomic Energy. The Accident at the Chernobyl' Nuclear Power Plant and its Consequences. Information compiled for the IAEA Expert's Meeting, 25-29 August 1986, Vienna, August 1986
2. International Atomic Energy Agency. Summary Report on the Post-Accident Review Meeting on the Chernobyl Accident, International Nuclear Safety Advisory Group, Safety Series No.75-INSAG-1, IAEA, Vienna, 1986.
3. International Atomic Energy Agency. Techniques and Decision Making in the Assessment of Off-Site Consequences of an Accident in a Nuclear Facility, IAEA Safety Guides, Safety Series No.86, IAEA, Vienna, 1987.
4. International Atomic Energy Agency. Dispersion Atmospheriques et choix des sites de centrales nucleaires: guide de surete. AIEA, Vienne, 1981. STI/PUB/549.

5. Vallario, E.J. Evaluation of Radiation Emergencies and Accidents. IAEA Technical Reports Series No.152. IAEA, Vienna, 1974.
6. Commissariat a l'Energie Atomique. Institut de protection et de Surete Nucleaire. L'Accident de Tchernobyl. Rapport IPSH No 2/86, Juin 1986.
7. Ursu, I. Physics and Technology of Nuclear Materials. Pergamon Press, Ltd., London, 1985.
8. Oncescu, M. Impactul centralelor nucleare asupra biosferei (NPP Impact on Biosphere). ICEFIZ Preprint, Măgurele 1987.
9. Galeriu,D., Pascovici, Gh., Oncescu, M. Sinopsis al măsurătorilor radiometrice din IFIN (Radiometric Measurements in IFIN - a Synopsis), ICEFIZ Preprint, Măgurele 1986.

Appendix 1 - Analytical Expressions for the Quantities Entering the Flight-Scan Table 1

$$\rho_{oj} = \frac{a}{16\pi^{\frac{3}{2}}\sqrt{D_x D_y D_z}} \cdot \frac{e^{\frac{v}{2D_x}X_o - \frac{v^2}{4D_x}t_j}}{t_j^{\frac{3}{2}}} \cdot \frac{\sqrt{\frac{D_x}{\beta}} + X_o}{X_o} \cdot e^{-\frac{1}{4t_j D_x}\left(\sqrt{\frac{D_x}{\beta}} + X_o\right)^2} \qquad j = 1,2,3 \tag{A.1.1}$$

$$\rho_{1j} = \frac{a}{16\pi^{\frac{3}{2}}\sqrt{D_x D_y D_z}} \cdot \frac{e^{\frac{v}{2D_x}(X_o+d) - \frac{v^2}{4D_x}t_j}}{t_j^{\frac{3}{2}}} \cdot \frac{\sqrt{\frac{D_x}{\beta}} + X_o + d}{X_o + d} \cdot e^{-\frac{1}{4t_j D_x}\left(\frac{D_x}{\beta} + X_o + d\right)^2} \qquad j = 1,2,3 \tag{A.1.2}$$

$$\rho_{2j} = \frac{a}{16\pi^{\frac{3}{2}}\sqrt{D_x D_y D_z}} \cdot \frac{e^{\frac{v}{2D_x}(X_o+2d) - \frac{v^2}{4D_x}t_j}}{t_j^{\frac{3}{2}}} \cdot \frac{\sqrt{\frac{D_x}{\beta}} + X_o + 2d}{X_o + 2d} \cdot e^{-\frac{1}{4t_j D_x}\left(\frac{D_x}{\beta} + X_o + 2d\right)^2} \qquad j = 1,2 \tag{A.1.3}$$

$$\rho'_{oj} = \frac{a}{16\pi^{\frac{3}{2}}.\sqrt{\beta}.\sqrt{D_x D_y D_z}} \cdot \frac{e^{\frac{v}{2D_x}x_o - \frac{v^2}{4D_x}t_j}}{t_j^{\frac{3}{2}}} \cdot \left(\sqrt{\beta} + \frac{1}{\sqrt{\frac{x_o^2}{D_x} + \frac{h^2}{D_z}}}\right) \cdot e^{-\frac{1}{4t_j}\left(\frac{1}{\sqrt{\beta}} + \sqrt{\frac{x_o^2}{D_x} + \frac{h^2}{D_z}}\right)^2} \qquad j = 1,2 \tag{A.1.4}$$

$$\rho''_{oj} = \frac{a}{16\pi^{\frac{3}{2}}.\sqrt{\beta}.\sqrt{D_x D_y D_z}} \cdot \frac{e^{\frac{v}{2D_x}x_o - \frac{v^2}{4D_x}t_j}}{t_j^{\frac{3}{2}}} \cdot \left(\sqrt{\beta} + \frac{1}{\sqrt{\frac{x_o^2}{D_x} + \frac{d^2}{D_y}}}\right) \cdot e^{-\frac{1}{4t_j}\left(\frac{1}{\sqrt{\beta}} + \sqrt{\frac{x_o^2}{D_x} + \frac{d^2}{D_y}}\right)^2} \qquad j = 1,2 \tag{A.1.5}$$

Appendix 2 - Analytical Expressions for the Quantities Entering the Flight-Scan Table 2

$$\rho_0 = \frac{a}{8\pi\sqrt{\pi\beta D_y D_z}} \cdot \frac{1}{X_o} \cdot \frac{e^{-\frac{1}{\beta\left(t-\frac{X_o}{v}\right)}}}{\left(t-\frac{X_o}{v}\right)^{\frac{3}{2}}} \cdot e^{-\frac{v}{4D_y}\frac{Y_o^2}{X_o}} \qquad \text{(A.2.1)}$$

$$\rho_0' = \rho_0 \cdot e^{-\frac{v}{4D_z}\frac{h^2}{X_o}} \qquad \text{(A.2.2)}$$

$$\rho_1 = \frac{a}{8\pi\sqrt{\pi\beta D_y D_z}} \cdot \frac{1}{X_o} \cdot \frac{e^{-\frac{1}{\beta\left(t-\frac{X_o}{v}\right)}}}{\left(t-\frac{X_o}{v}\right)^{\frac{3}{2}}} \cdot e^{-\frac{v}{4D_y}\frac{(Y_o+d)^2}{X_o}} \qquad \text{(A.2.3)}$$

$$\rho_2 = \frac{a}{8\pi\sqrt{\pi\beta D_y D_z}} \cdot \frac{1}{X_o} \cdot \frac{e^{-\frac{1}{\beta\left(t-\frac{X_o}{v}\right)}}}{\left(t-\frac{X_o}{v}\right)^{\frac{3}{2}}} \cdot e^{-\frac{v}{4D_y}\frac{(Y_o+2d)^2}{X_o}} \qquad \text{(A.2.4)}$$

$$\rho_3 = \frac{a}{8\pi\sqrt{\pi\beta D_y D_z}} \cdot \frac{1}{X_o+d} \cdot \frac{e^{-\frac{1}{\beta\left(t-\frac{X_o+d}{v}\right)}}}{\left(t-\frac{X_o+d}{v}\right)^{\frac{3}{2}}} \cdot e^{-\frac{v}{4D_y}\frac{Y_o^2}{X_o+d}} \qquad \text{(A.2.5)}$$

$$\rho_3' = \rho_3 \cdot e^{-\frac{v}{4D_z}\frac{h^2}{X_o+d}} \qquad \text{(A.2.6)}$$

$$\rho_4 = \frac{a}{8\pi\sqrt{\pi\beta D_y D_z}} \cdot \frac{1}{X_o+d} \cdot \frac{e^{-\frac{1}{\beta\left(t-\frac{X_o+d}{v}\right)}}}{\left(t-\frac{X_o+d}{v}\right)^{\frac{3}{2}}} \cdot e^{-\frac{v}{4D_y}\frac{(Y_o+d)^2}{X_o}} \qquad \text{(A.2.7)}$$

FIGURE CAPTIONS

Fig.1 Reference frames to describe cloud dispersal; $\bar{v}$ is the dominant wind velocity. SS -- the Source System (X,Y,Z); CS -- the Cloud System (x,y,z); v.eqs.(2.1,2).

Fig.2 Time-profile of the generic Green function (2.33).

Fig.3 Time-profiles of the analytical part of the model-source strength (3.1), chosen to describe 3-dimensional protracted diffusion. The lower the wind, the weaker the depletion at source, and consequently -- the more prolonged the emission. The absolute maxima: A -- 177656.72 Ci/(km^3.h); B -- 230864.58 Ci/(km^3.h).

Fig.4 Cloud patterns, assuming a 3-dimensional diffusion (v.eq.(3.1.19) without its last, reflexion, term). Horizontal sections into the clouds, at centreline altitude. A -- lines of equal concentration at 65 hours into the release time; B -- evolvment in time of the 100 pCi/m^3 line of equal concentration. Dotted area: the 65-hour cloud, as detailed in A.

Fig.5 Time-profiles of the air-borne activity concentration, assuming a 3-dimensional diffusion (v.eq.(3.1.19), reflection neglected); A -- at different altitudes, on the vertical of the same spot beneath centreline; B -- at different spots (distances from source), downwind the cloud centreline. The absolute maxima: A -- 59278 pCi/m^3; B -- 46295 pCi/m^3.

Fig.6 Time-profile of the analytical part of the model-source strength (3.2.1), chosen to describe 2-dimensional protracted diffusion. Persistence of emission depends, naturally, only on the blast factor, β. Case A, to be compared with case E in fig.3, confirms the convergence of the 3-d and 2-d mode.-sources at very low winds. The absence of the downwind diffusion ($D_x \to 0$) provides for prolonged cloud persistence. The absolute maxima: A -- 230864.58 Ci/(km^3.h); B -- 57810.96 Ci/(km^3.h).

Fig.7 Cloud patterns, assuming a 2-dimensional diffusion (v.eq.(3.2.13), reflection neglected). Horizontal sections into the clouds, at centreline altitude. A -- lines of equal concentration at 65 hours into the release time; B -- evolvment in time of the 100 pCi/m^3-line of equal concentration. Dotted area: the 65-hour cloud, as detailed in A.

Fig.8 Time-profiles of the air-borne activity concentration assuming a 2-dimensional diffusion (v.eq.(3.2.13), reflection neglected); A -- at different altitudes on the vertical of the same spot beneath centreline; B -- at different spots (distances from source), downwind the cloud centreline. Note sharper strikes in comparison with the 3d-model (v.fig.5). The absolute maxima: A -- 57926 pCi/m^3; B -- 116041 pCi/m^3.

Fig.9 Goniometry of a direct blow. The small circles indicate the five airborne measuring units heading cross-wind, at a moment appropriate for air sampling. The star locates the virtual centre of dispersion, at the elevation H above source. For the notations refer to paragraph 4.1.

Fig.10 Goniometry of an indirect blow. The cloud centreline does not cross the readily accessible territory (shaded area). The small circles indicate the seven airborne measuring units, heading cross-wind, at the moment of air-sampling. The star locates the virtual centre of dispersion, at the elevation H above source. For the notations refer to paragraph 4.2.

NOTE on the units

The following units apply to the quantities in the figures:

- Lengths: X, Y, Z, x, y, z, H, h, d, ξ, ...	kilometres (km)
- Time: t, ...	on abscissas -- days (d) in calculations and derived quantities -- hours
- Wind velocity: v	kilometres/hour (km/h)
- Wind direction: u	radians (rad)*
- Diffusion coefficients: D_x, D_y, D_z.....	square kilometres/hour (km^2/h)
- Activity: a , ...	Curie (Ci)
- Activity concentrations, ρ , ...	pico-Curie/cubic metre (pCi/m^3)
- Source strengths, a(X,Y,Z;t), ...	Curie/(cubic kilometre. hour) ($Ci/(km^3.h)$)
- Blast factors, β , ...	1/second (s^{-1})

*The computer code at the origin of figures 2 through 8 has uniformly used u = π/2 rad, from North by E; ., in a third system of coordinates, beside SS and CS -- the Map System -- that is to be sized according to the graphic capabilities available.

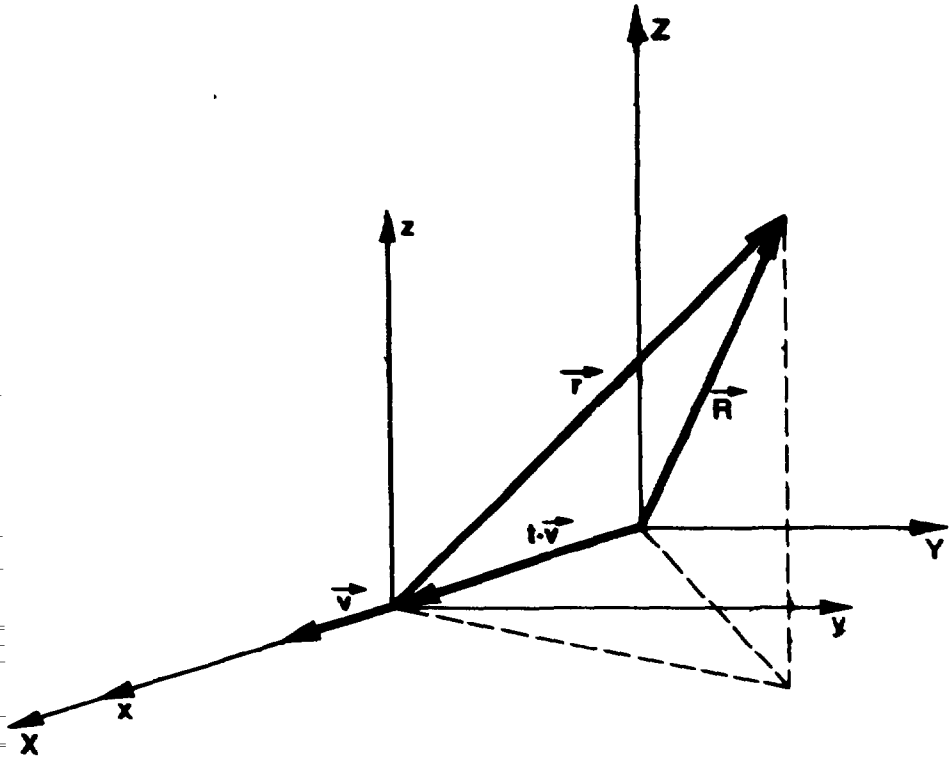

Fig. 1

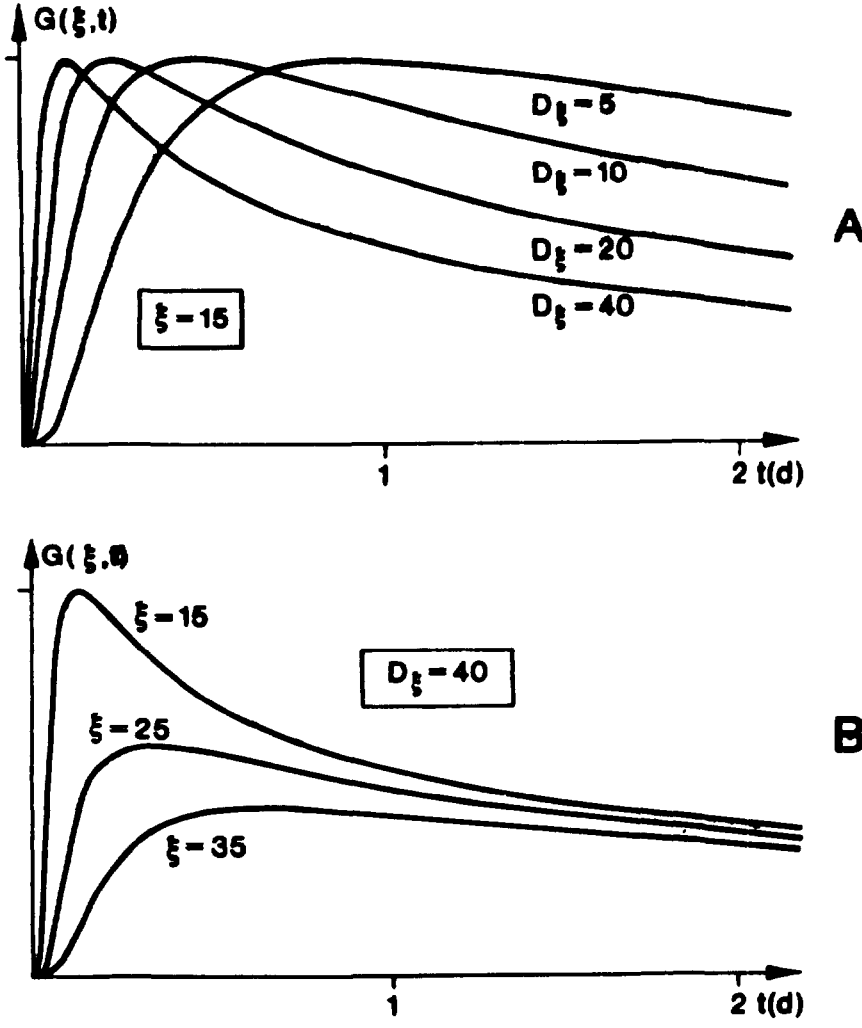
G(ξ,t)
$D_\xi = 5$
$D_\xi = 10$
$D_\xi = 20$
$D_\xi = 40$
ξ = 15
A
1
2 t(d)
G(ξ,t)
ξ = 15
$D_\xi = 40$
ξ = 25
ξ = 35
B
1
2 t(d)

Fig. 2

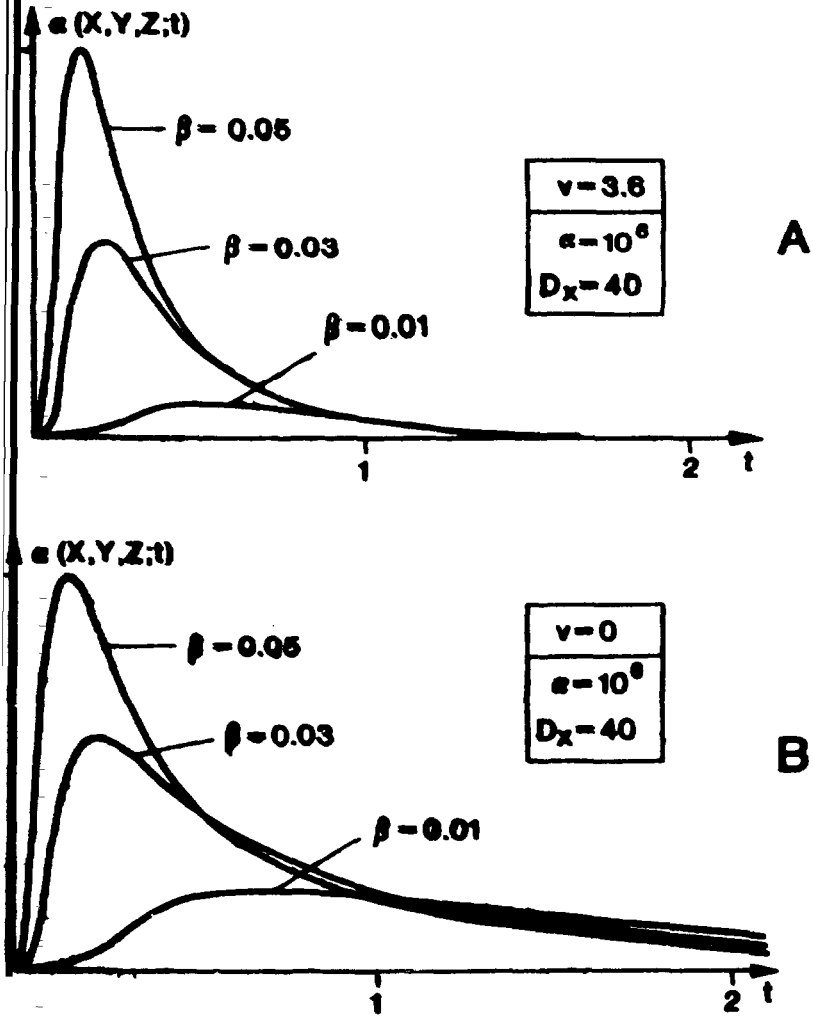
c (X,Y,Z;t)
β = 0.05
β = 0.03
β = 0.01
v = 3.6
α = 10^6
D_X = 40
A
1
2
t
c (X,Y,Z;t)
β = 0.05
β = 0.03
β = 0.01
v = 0
α = 10^6
D_X = 40
B
1
2
t

Fig. 3

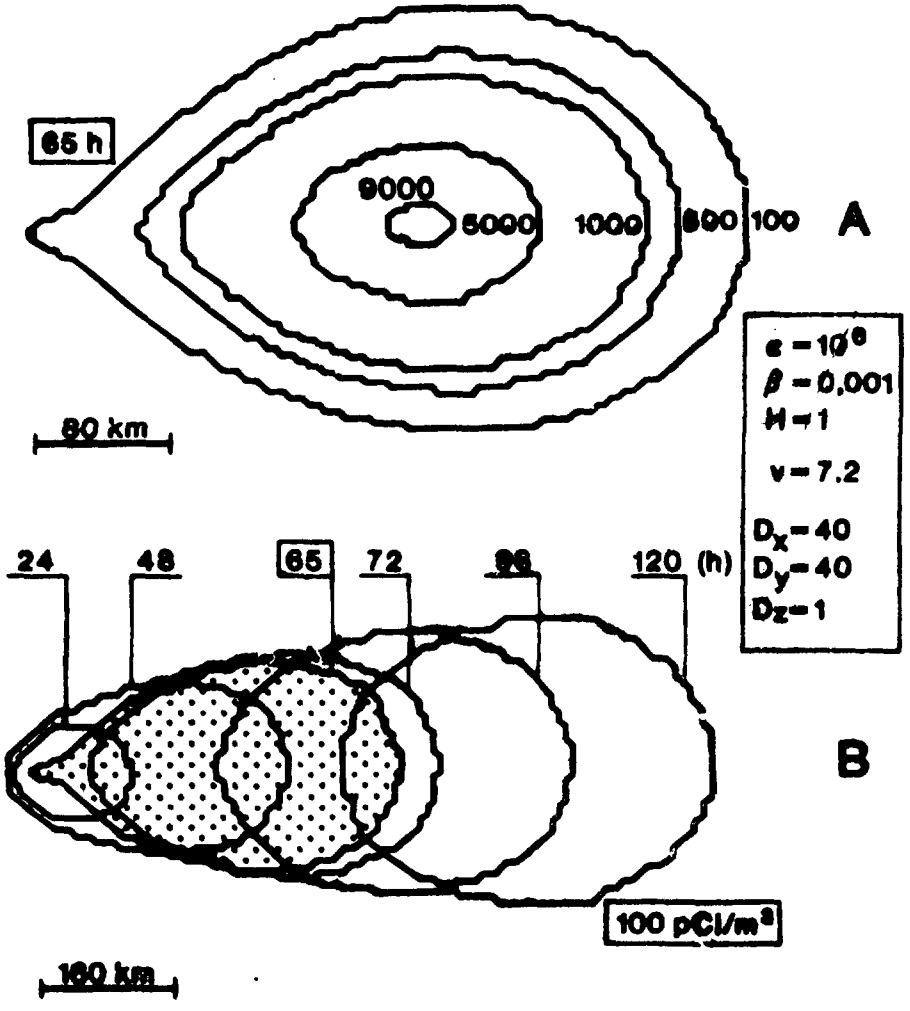
65 h
9000
5000
1000
800
100
A
80 km
$\varepsilon = 10^{6}$
$\beta = 0{,}001$
$H = 1$
$v = 7.2$
$D_x = 40$
$D_y = 40$
$D_z = 1$
24
48
65
72
96
120 (h)
B
100 pCi/m³
160 km

Fig.4

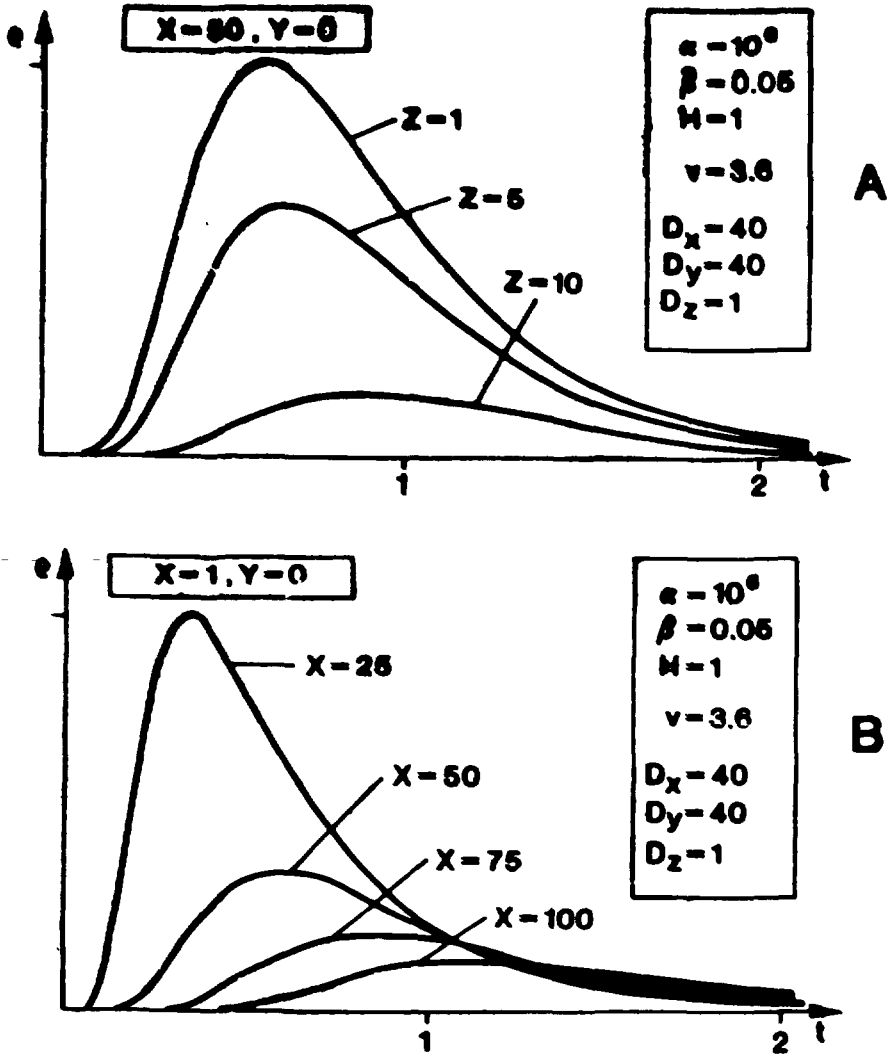
X=50, Y=0
Z=1
Z=5
Z=10
α=10⁶
β=0.05
M=1
v=3.6
Dx=40
Dy=40
Dz=1
A
X=1, Y=0
X=25
X=50
X=75
X=100
α=10⁶
β=0.05
M=1
v=3.6
Dx=40
Dy=40
Dz=1
B
1
2
t

Fig. 5

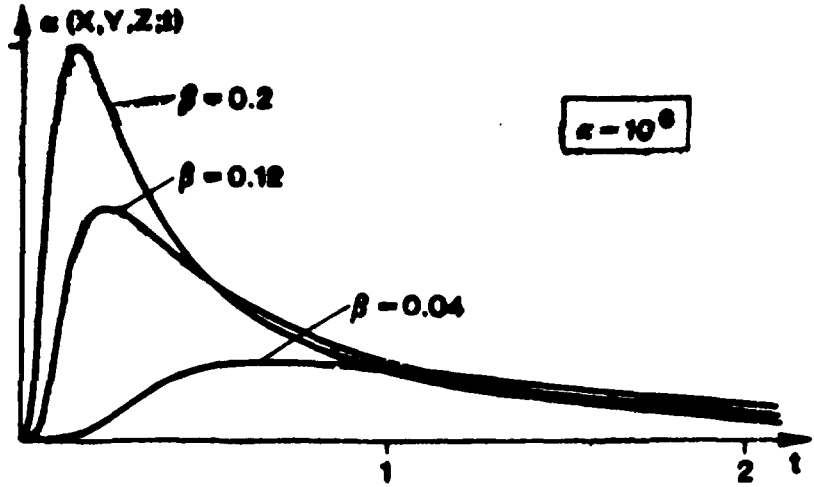

A

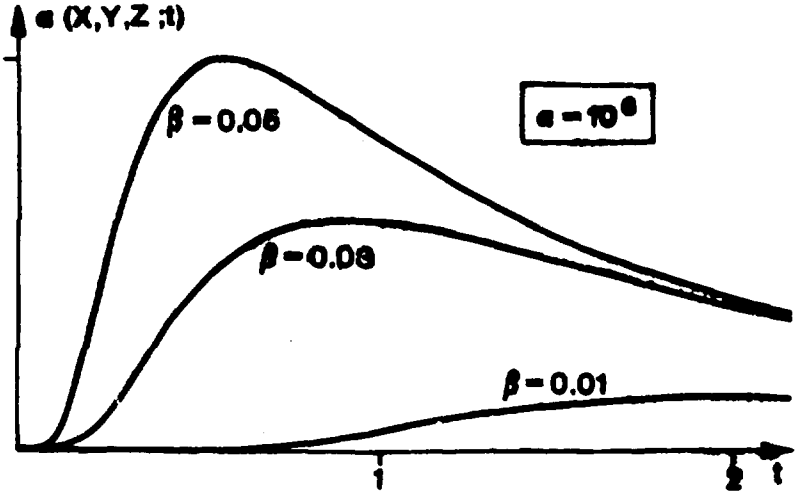

B

Fig.6

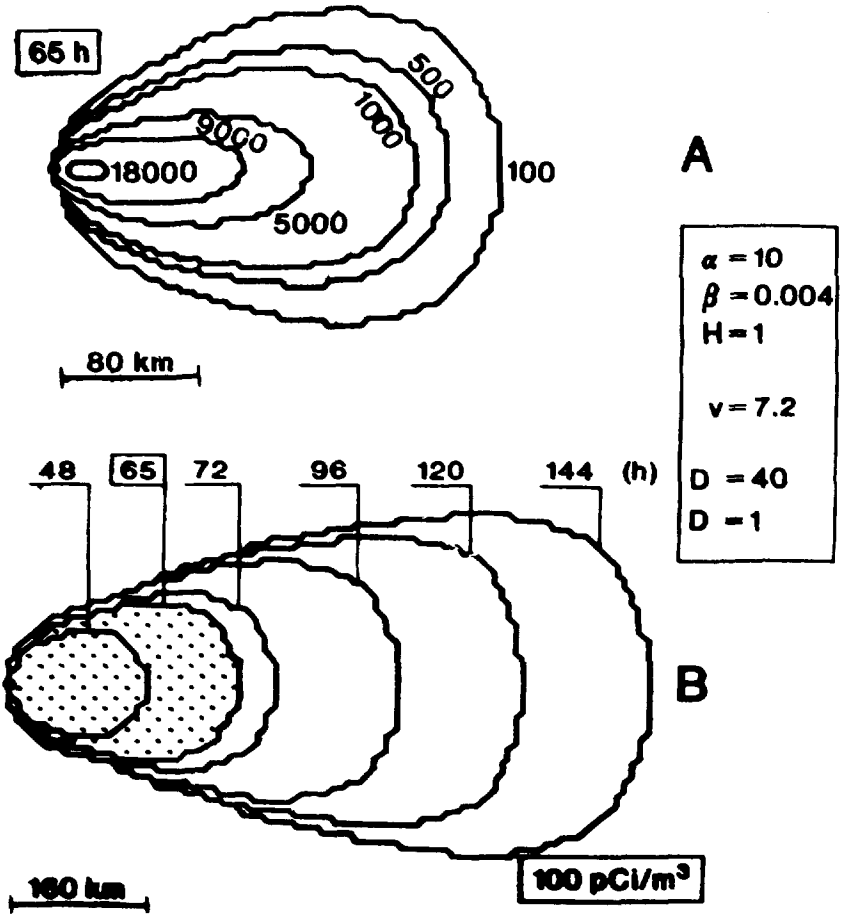
65 h
500
1000
9000
18000
5000
100
A
80 km
α = 10
β = 0.004
H = 1
v = 7.2
D = 40
D = 1
48
65
72
96
120
144
(h)
B
160 km
100 pCi/m³

Fig. 7

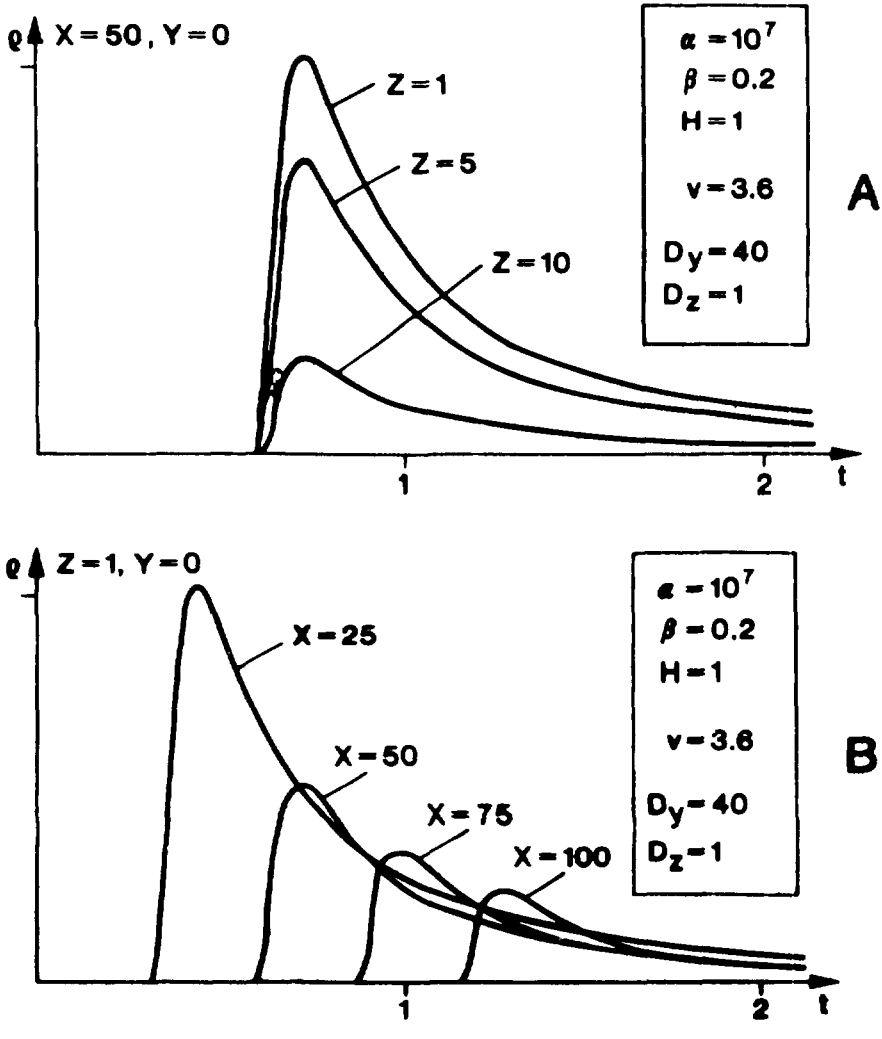
ϱ
X = 50, Y = 0
Z = 1
Z = 5
Z = 10
α = 10^7
β = 0.2
H = 1
v = 3.6
Dy = 40
Dz = 1
A
1
2
t
ϱ
Z = 1, Y = 0
X = 25
X = 50
X = 75
X = 100
α = 10^7
β = 0.2
H = 1
v = 3.6
Dy = 40
Dz = 1
B
1
2
t

Fig. 8

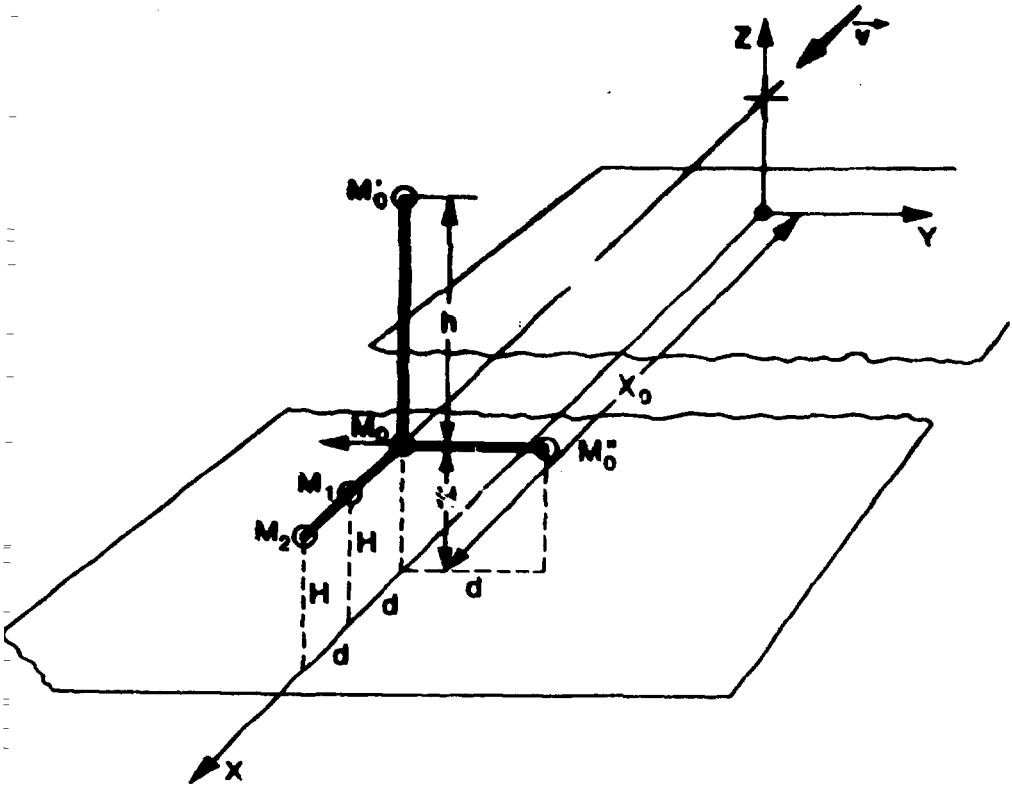

Fig. 9

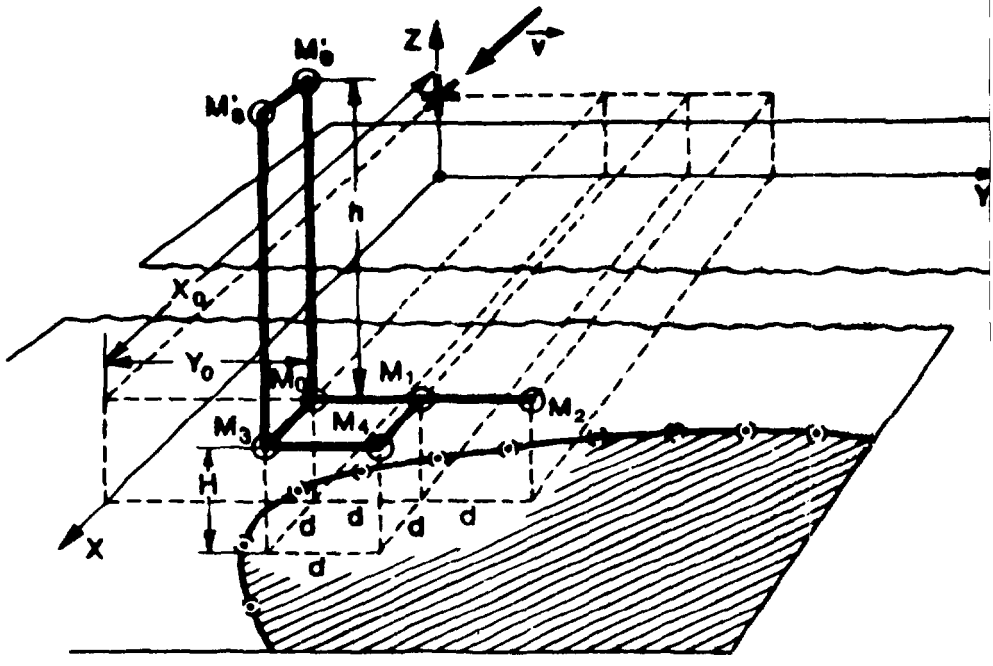

Fig. 10